Appl. Phys. B 68, 959–966 (1999) / DOI 10.1007/s003409901495

Applied Physics B
Lasers
and Optics

Multiline coherent oscillation in photorefractive crystals with two species of movable carriers

A. Shumelyuk[1], **S. Odoulov**[1,*], **G. Brost**[2]

[1] Institute of Physics, National Academy of Sciences, 252 650 Kiev, Ukraine
(E-mail: odoulov@iop.kiev.ua)
[2] Air Force Research Laboratory/SNDR 25 Electronic Pkwy, Rome, NY 13441-4515, USA

Received: 12 November 1998/Revised version: 11 January 1999/Published online: 7 April 1999

Abstract. The coherent oscillation, because of nearly degenerate four-wave mixing in photorefractive crystals with two types of movable charge carriers, occurs at two spectral lines symmetrically shifted with respect to the pump frequency. Consequently the output oscillation exhibits the high contrast intensity modulation. The frequency separation of two oscillation modes (and modulation frequency of the output intensity) depend on the incident light intensity and spatial frequency of the developing grating. A model is presented explaining this type of oscillation by the two-maxima shape of the gain spectrum in crystals with sufficiently different relaxation times of two space-charge gratings, one formed by movable electrons and the other one by movable holes. The experimental data for coherent oscillator with tin hypothiodiphosphate ($Sn_2P_2S_6$) are in reasonable quantitative agreement with the calculations.

PACS: 42.65Yj; 42.65Sf; 42.65Hw

Quite often a coherent light used for the recording of photorefractive grating excites two types of movable carriers, the holes and electrons, simultaneously. After the pioneering work of E. Krätzig proving the possibility to switch from the dominant electron photoconductivity to hole conductivity in iron-doped $LiNbO_3$ by the thermal treatment of the sample in oxygen atmosphere [1, 2] an abundance of publications appeared, experimental (see, for example, [3–6]) as well as considering theoretically the consequences of electron/hole competition (see, for example, [7–10]). All these and other related works resulted in the rather pessimistic general conclusion that the formation of two gratings, one via the redistribution of the photoexcited electrons and the other via the motion of the holes, inhibits the steady-state refractive index change (and therefore gain factor and diffraction efficiency) because these two gratings are π out of phase with each other.

Only one exception exists to our knowledge, which is the successful exploration of the so-called temperature-intensity resonance in semiconductors [11, 12]. By working in an external electric field in carefully selected conditions (photorefractive material with special parameters, well-adjusted temperature, intensity, polarization, and angle of incidence of the recording waves, etc.) it becomes possible to change the mutual phase shift of the two gratings from π to less than $\pi/2$ and ensure in such a way the constructive interference. The advantage of this technique is that it provides automatically the $\pi/2$ phase shift of the resulting phase grating with respect to the light fringes even in a moderate dc electric field. The best published result is the enhancement of the gain factor in InP:Fe crystal up to 31 cm^{-1} in 10 KV/cm electric field [12].

In the present article we analyse a specific kind of electron/hole competition in photorefractive crystals, with considerably different (several orders of magnitude) dielectric relaxation times for electron and hole subsystems. It has been shown in our previous publications [13, 14] that different four-wave mixing processes with nearly (but not exactly) degenerate frequencies of interacting waves can be at least as effective as in the single-carrier case. Now we report on particular properties of the coherent oscillators (photorefractive lasers) using these materials.

1 Experiment

Tin hypothiodiphosphate ($Sn_2P_2S_6$, SPS) [13–16] is chosen as a typical crystal with two types of movable carriers. The existence of two gratings with strongly different decay times (from seconds to milliseconds for the fast grating and from minute to several minutes for the slow one) was revealed both in the dynamics of the two-beam coupling [15] and diffraction efficiency [16]. The crystals are sensitive in the red and near-infrared region of the spectrum [17]; in the present work the He-Ne laser light is used to get the largest possible photorefractive response. All measurements are performed with the sample K3 (type 1 [17]) of tin hypothiodiphosphate; the

* Like many other colleagues I benefited enormously during my visits to Osnabrück from the stimulating, creative and friendly atmosphere created by Prof. Dr. Eckard Krätzig in his laboratory. Thanking him for his gracious hospitality it is a great pleasure to wish him, one of the fathers and universally recognized leaders in the physics of photorefraction, a very happy 60th birthday.

results with other samples exhibiting pronounced electron–hole competition (type 1) are qualitatively similar.

1.1 Amplification of coherent light waves

The traditional two-beam coupling geometry (Fig. 1) was used to study the amplification of a weak signal wave in the presence of the strong pump wave. The output beam from a He-Ne laser (0.63 μm, TEM_{00}, linearly polarized in the plane of drawing) is split into two beams recording a holographic grating in SPS sample. The signal-to-pump intensity ratio is about 1:1000. When the pump wave is sent to the sample in addition to the weak signal wave the intensity of the signal wave increases rapidly reaching the maximum value which is 180 times higher than the initial one. With further illumination the intensity of the amplified wave is decreasing slowly, saturating at a value which is 45 times smaller than the peak value. Qualitatively the dynamics of the two-beam coupling at $\lambda = 0.63\,\mu m$ is similar to that at $\lambda = 1.06\,\mu m$ [16] for SPS samples of type 1 [17] thus proving the formation of two out-of-phase space-charge gratings, one formed by movable electrons and other formed by movable holes.

Figure 2 shows the grating spacing dependence of the maximum transient gain factor. The data are corrected for incomplete overlap of the finite-size recording beams with Gaussian intensity distribution (see Appendix in [16]). More than 7 cm^{-1} gain factor is reached for grating spacing close to the Debye screening length $\ell_s \approx 1.5$–$2\,\mu m$. For the sample thickness $\ell = 9$ mm the coupling strength is $\Gamma\ell \approx 5.4$, i.e., is larger than the threshold coupling strength for nearly all known photorefractive coherent oscillators (providing negligible cavity losses).

The dynamics of the build-up of each of the two space-charge gratings is nearly exponential; the grating spacing dependences for the characteristic relaxation time of the electron and hole gratings are shown in Fig. 3a,b, respectively. The relaxation time constants are evaluated from the beam-coupling experiments with the overall intensity in the sample $I_0 = 3\,W/cm^2$.

From the comparison with the theory of space-charge grating formation [24] the conclusion follows that for the electron (fast) grating the Debye screening length is larger

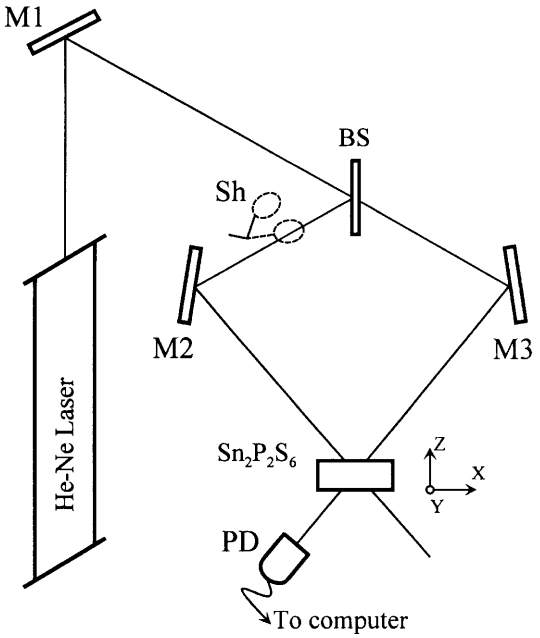

Fig. 1. Schematic representation of the experimental setup for the study of the two-beam coupling. M1–M3 are the mirrors, BS is the beam splitter, Sh is the shutter, and PD is the photodetector

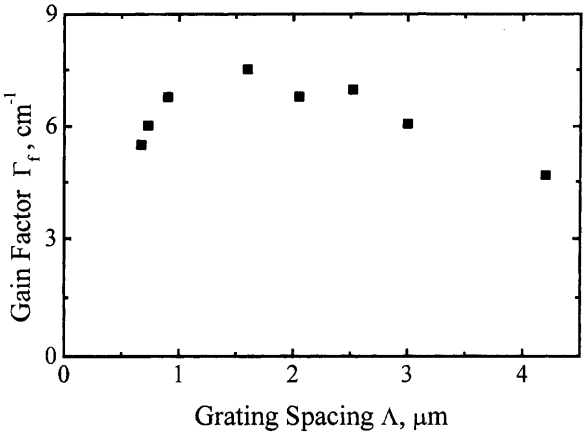

Fig. 2. Grating-spacing dependence of the transient gain factor. Total light intensity in the sample is $I_0 = 3\,W/cm^2$

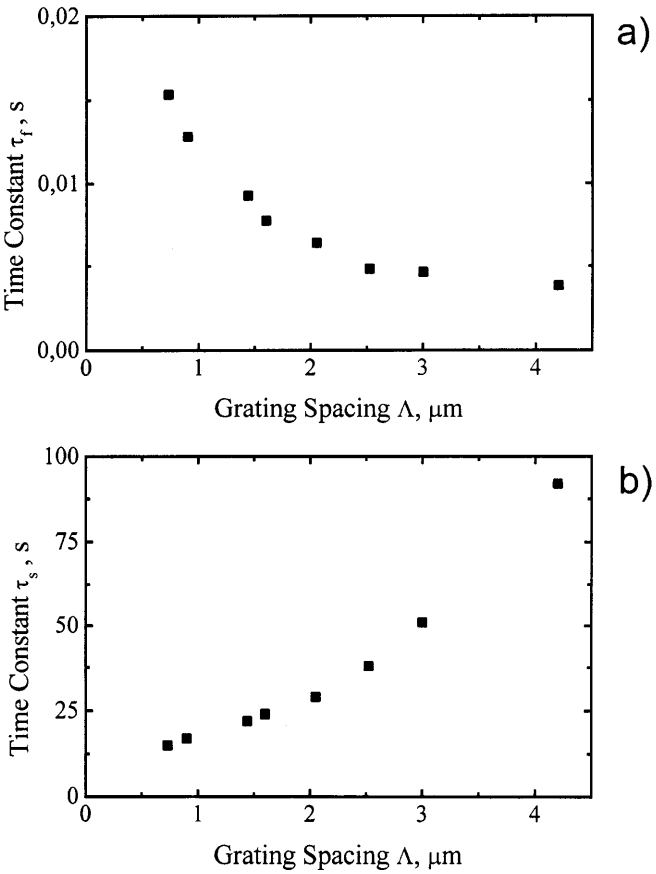

Fig. 3a,b. Grating-spacing dependence of characteristic relaxation time for the fast grating (**a**) and slow grating (**b**) for the intensity of interacting waves $I_0 = 3\,W/cm^2$

than the diffusion length whereas the opposite relationship holds for the hole (slow) grating. The data of Figs. 2 and 3 can be used also for evaluation of the characteristic transport lengths (Debye screening length, diffusion length) and effective trap densities.

1.2 Coherent oscillation in ring-loop geometry

Figure 4 represents schematically the experimental setup for the study of the coherent oscillation. The pump wave transmitted through the sample is reflected back by the mirrors M3 and M5. In such a way the ring-loop oscillator [18] is built. The length of the loop is usually larger than the coherence length of the laser (≈ 15 cm) to exclude the possibility of the reflection gratings recording in SPS. Mirrors M3 and M5 can be repositioned in such a way that the angle of the loop near the sample can vary from 5° to 45°. The beam splitter M4 and the additional mirror M2 with the receiver PD and apertures D1 and D2 are used to record the beat-frequency mark for evaluation of the frequency shift. When shutter Sh cuts the beam from mirror M2 the detector PD measures the output intensity of the coherent oscillator as is. When this shutter is open a coherent reference wave (with the frequency of the pump wave ω, local oscillator) is coming to the detector in addition to the oscillation wave and the frequency beat signature is registered. The variable beam attenuator, VBA, put in the front of the laser allows for the intensity control of the beam incident upon the sample. All the data are stored in the memory of the computer; the processing of data (Fourier transform, etc.) is also done with the same computer.

Figure 5 shows the typical dynamics of the oscillation intensity. Before the exposure is started ($t \leq 0$) all the photorefractive gratings inside the sample are erased with the incoherent illumination (the light of a 100-W halogen lamp transported to the sample with the flexible bunch of waveguides). At t = 0 the pump beam starts to illuminate the sample. The onset of oscillation occures with a certain time delay after the beginning of the exposure (a manifestation of the optical phase transition [19]), but in the time scale shown in Fig. 5 this delay is indistinguishable. The Fourier spectrum of the developed periodic modulation of the oscillation intensity in the steady state is shown in Fig. 6a. The most pronounced peak ($\approx 6.3 \pm 0.15$ Hz) corresponds to the main modulation frequency, however the other well-defined

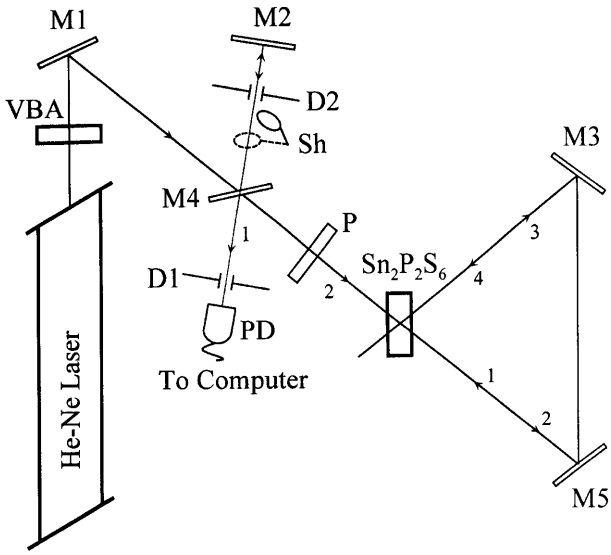

Fig. 4. Schematic representation of the photorefractive ring-loop coherent oscillator. M1–M5 are the mirrors, M4 is the beam splitter, PD is the photodetector, Sh is the shutter, D1, D2 are the apertures, VBA is the variable beam splitter

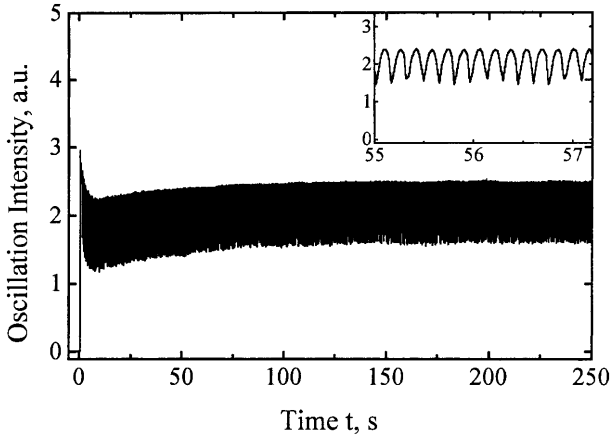

Fig. 5. Temporal variations of the oscillation intensity for the incident pump intensity $I_p = 3\,\mathrm{W/cm^2}$ and grating spacing $\Lambda = 0.9\,\mu\mathrm{m}$

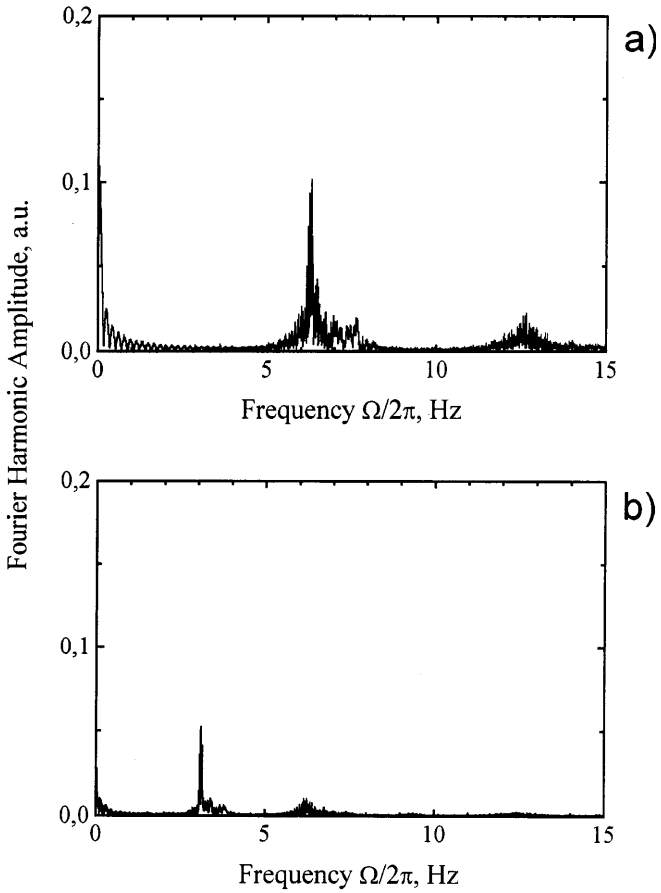

Fig. 6a,b. Fourier spectra. (**a**) Temporal variations of the oscillation intensity. (**b**) Beat frequency mark (oscillation wave plus a part of the pump wave)

frequencies are present, too, for example, second harmonic of the principal frequency, ($\approx 12.6 \pm 0.5$ Hz). Figure 6b represents the spectrum of the beat frequency when both the oscillation and reference waves are coming to the detector. It is easy to note the appearance of the additional peak ($\approx 3.1 \pm 0.1$ Hz) with high amplitude and roughly half frequency-detuning as compared to the main peak in the oscillation spectrum. The two-times difference between the frequency of the beat-frequency mark and frequency of output intensity modulation was observed for all spatial frequencies of the grating self-developing in the sample. This proves that the oscillation consists of two modes symmetrically shifted in frequency with respect to the frequency of the pump wave.

The modulation frequency in the oscillation spectrum is a function of the input intensity (Fig. 7). This might be expected as the characteristic time of photorefractive grating build-up depends on photoconductivity. It should be noted however that it is not a trivial linear dependence previously observed for other coherent oscillators with shifted frequencies (see, for example, [20]).

For high intensities of the pump wave a pronounced self-focusing has been observed in the investigated sample. The intensity of the pump beam reflected into the sample by the cavity mirrors was drastically increasing leading to the superlinear growth of the measured modulation frequency. That is why, to measure the intensity dependence of the frequency detuning (Fig. 7), a short cavity (≈ 5 cm) was used with the intensity of the pump wave below 2 W/cm^2. As the focal length of the nonlinear (thermal) lens inside the sample is much longer than the cavity length the reflected beam size remains roughly the same when the intensity of the incident beam is decreasing. This means that the total intensity inside the sample is linearly related to the input intensity which makes easy the comparison with the theory. The recording of the reflection gratings mentioned above reduces the efficiency of oscillation but in zero approximation does not affect the shape of the gain spectrum itself, therefore a qualitative comparison with calculation is possible.

By modifying the angle of the loop it is possible to change the frequency separation between the oscillation modes (Fig. 8). These changes are, however, relatively small: The

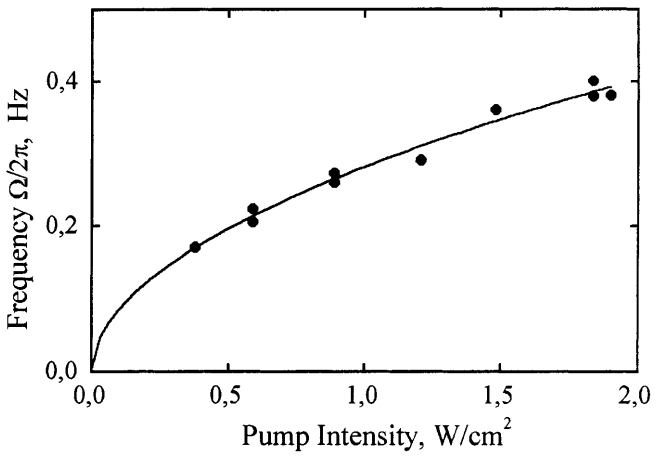

Fig. 7. Pump-intensity dependence of the oscillation frequency; grating spacing $\Lambda = 1.7$ μm

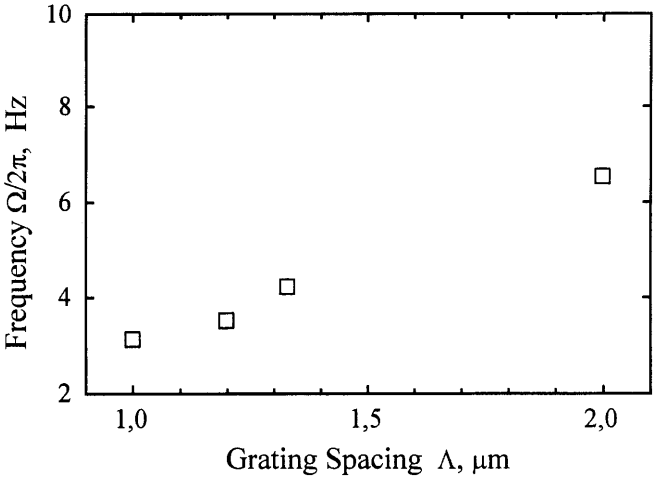

Fig. 8. Spatial frequency dependence of the oscillation frequency

detuning frequency becomes approximately doubled when the grating spacing is increasing from 1 to 2 μm.

The oscillation with shifted frequency has been already observed in different oscillator geometries [20, 21] but the stable two-mode steady-state operation is reported, to our knowledge, for the first time. It will be clear from the following sections that two modes are related here to excitation of the transmission grating with exactly the same grating vector $\boldsymbol{K}$; this is not a consequence of competition of gratings in different partially overlapping sample area [22] or gratings with different structures (different $\boldsymbol{K}$-vectors) [23].

2 Calculations

To describe the coherent oscillator based on nonlinear wave mixing one should know how the complex amplitude of the signal wave after single pass through the crystal changes, i.e., to what extent a weak signal is amplified and how large is the nonlinear phase shift of the amplified wave. These values are usually calculated by solving the nonlinear wave equation (coupled-wave analysis) with the complex coupling constant extracted from the solution of the material equations (see, for example, [24]).

In photorefractive materials the refractive index changes because of the formation of the space-charge: the electric field of this space-charge affects the refractive index via the linear electrooptic effect. For the scalar nonlinear mixing (all waves have identical polarization) the coupling constant is

$$\gamma = \pi i n^3 r_{\mathrm{eff}} E_{\mathrm{sc}} / m\lambda \,, \tag{1}$$

where n is the refractive index, r_{eff} is the effective electrooptic constant, λ is the light wavelength, m is the recording fringe contrast, and E_{sc} is the space charge field; it is a complex value which takes into account possible spatial shift of the index grating with respect to the recording light fringes.

In Sect. 2.1 the solution of the material equations for the complex coupling strength is presented. In Sect. 2.2 the threshold conditions of oscillation are discussed using the analysis of the gain spectrum and phase coupling constant spectrum for nearly degenerate in frequency oscillation.

2.1 Gain factor and phase coupling coefficient

Suppose two waves,

$$E_1 = A_1 \exp(-i\boldsymbol{k}_1 \cdot \boldsymbol{r} + i\omega t),$$
$$E_2 = A_2 \exp(-i\boldsymbol{k}_2 \cdot \boldsymbol{r} + i(\omega + \Omega)t), \quad (2)$$

impinge upon a photorefractive sample, forming a running fringe pattern

$$I = I_0 \left[1 + m \exp(iKx + i\Omega t)\right]. \quad (3)$$

Here $\boldsymbol{k}_{1,2}$ are the wavevectors of the recording waves, ω and $(\omega+\Omega)$ are their temporal frequencies, $I_0 = |A_1|^2 + |A_2|^2$ is the total intensity inside the crystal, the fringe contrast is $m = |2A_1A_2|/I_0$, and K is the spatial frequency of the fringe pattern. The contrast of the fringes is taken to be small, i.e., $m \ll 1$. The self-diffraction from the recorded grating is neglected, i.e., m is assumed to be independent of propagation coordinate z inside the sample. Therefore only the material equations are considered.

Two types of the impurity centers are assumed to be present, one with the energy level close to the conduction band and total density N_1 and the other close to the valence band with total density N_2. The first level is populated by electrons while the second is populated by holes. Both levels are partially ionized, N_1^{i} and N_2^{i} being the densities of the empty electron and hole levels, respectively. The electrons from level 1 can be excited to the conduction band thermally (with the probability β_{n}) or because of phototransition (with the probability $s_{\mathrm{n}}I$). Similarly, the holes can be released from level 2 to the valence band by thermal transition (probability β_{p}) or by phototransition (probability $s_{\mathrm{p}}I$).

The rate equations for ionized electron traps and hole traps are as follows [20]

$$\frac{\partial N_1^{\mathrm{i}}}{\partial t} = (\beta_{\mathrm{n}} + s_{\mathrm{n}}I)(N_1 - N_1^{\mathrm{i}}) - \gamma_{\mathrm{n}} N_1^{\mathrm{i}} n,$$
$$\frac{\partial N_2^{\mathrm{i}}}{\partial t} = -(\beta_{\mathrm{p}} + s_{\mathrm{p}}I) N_2^{\mathrm{i}} + \gamma_{\mathrm{p}}(N_2 - N_2^{\mathrm{i}})\, p, \quad (4)$$

where n and p are the densities and $\gamma_{\mathrm{n,p}}$ are the recombination constants for free electrons and free holes, respectively.

Continuity equations for electrons and holes are

$$\frac{\partial n}{\partial t} = \frac{\partial N_1^{\mathrm{i}}}{\partial t} + \frac{1}{e}\frac{\partial j_{\mathrm{n}}}{\partial x},$$
$$\frac{\partial p}{\partial t} = -\frac{\partial N_2^{\mathrm{i}}}{\partial t} - \frac{1}{e}\frac{\partial j_{\mathrm{p}}}{\partial x}, \quad (5)$$

and current equations are

$$j_{\mathrm{n}} = e\mu_{\mathrm{n}} n E + eD_{\mathrm{n}}\frac{\partial n}{\partial x},$$
$$j_{\mathrm{p}} = e\mu_{\mathrm{p}} p E - eD_{\mathrm{p}}\frac{\partial p}{\partial x}, \quad (6)$$

where $\mu_{\mathrm{n,p}}$ are the mobilities and $D_{\mathrm{n,p}} = (k_{\mathrm{B}}T/e)\mu_{\mathrm{n,p}}$ are the diffusivities for electrons and holes, respectively, while $j_{\mathrm{n,p}}$ are the electron and hole currents.

The Poisson equation completes the set of material equations for calculation of the space charge field

$$\frac{\partial E}{\partial x} = \frac{e}{\epsilon\epsilon_0}\left(p - n + N_1^{\mathrm{i}} - N_2^{\mathrm{i}} - N_{\mathrm{a}}\right), \quad (7)$$

where $\epsilon\epsilon_0$ is the dielectric constant and N_{a} is the density of optically inactive acceptors which are compensating for N_1^{i} and N_2^{i}.

The material equations (4)–(7) have been solved in [14] and the space-charge distribution E_{sc} was calculated. In [14] we were interested in calculation of temporal development of the gain factor Γ, i.e., the real part of the coupling constant, $\Gamma = 2\,\mathrm{Re}\{\gamma\}$ to describe the measured dynamics of nearly degenerate two-beam coupling [13]. In the present paper we are interested in steady-state values of Γ and also of the imaginary part $\Psi = \mathrm{Im}\{\gamma\}$ of the coupling constant

$$\Psi = \mathrm{Im}\left\{(\pi i n^3 r_{\mathrm{eff}} E_{\mathrm{sc}})/m\lambda\right\}, \quad (8)$$

which defines the nonlinear phase shift of the wave diffracted from the moving grating.

The results presented below are obtained with the following restrictions, well justified for SPS crystals [15, 16]: (i) the relaxation time for the fast grating is considered to be much smaller than that of the slow grating; (ii) the carriers involved in formation of the slow grating are assumed to be thermally generated whereas the formation of the fast grating is the photostimulated process; and the saturation regime is considered. Within these approximations

$$\Gamma = -\frac{2\pi n^3 r_{\mathrm{eff}} E_D}{\lambda}\left[\frac{1 + l_{\mathrm{Sn}}^2 K^2}{(1 + l_{\mathrm{Sn}}^2 K^2)^2 + (\tau_m^{\mathrm{n}}\Omega)^2(1 + l_{Dn}^2 K^2)^2}\right] \times \left[1 - \frac{1 + l_{\mathrm{Sp}}^2 K^2}{(1 + l_{\mathrm{Sp}}^2 K^2)^2 + (\tau_m^{\mathrm{p}}\Omega)^2(1 + l_{Dp}^2 K^2)^2}\right], \quad (9)$$

$$\Psi = \frac{\pi n^3 r_{\mathrm{eff}} E_{\mathrm{D}}}{\lambda}\left[\frac{1 + l_{\mathrm{Sn}}^2 K^2}{(1 + l_{\mathrm{Sn}}^2 K^2)^2 + (\tau_m^{\mathrm{n}}\Omega)^2(1 + l_{Dn}^2 K^2)^2}\right] \times \left[\frac{2\Omega\tau_m^{\mathrm{n}}(1 + l_{Dn}^2 K^2)}{1 + l_{\mathrm{Sn}}^2 K^2} - \frac{1 + l_{\mathrm{Sp}}^2 K^2}{(1 + l_{\mathrm{Sp}}^2 K^2)^2 + (\tau_m^{\mathrm{p}}\Omega)^2(1 + l_{Dp}^2 K^2)^2} \times \frac{2\Omega\tau_m^{\mathrm{p}}(1 + l_{Dp}^2 K^2)}{1 + l_{\mathrm{Sp}}^2 K^2}\right], \quad (10)$$

where $E_{\mathrm{D}} = K(k_{\mathrm{B}}T)/e$ is the diffusion length, k_{B} is Bolzmann constant, e is the electron charge, and T is the absolute temperature. The characteristic transport lengths are

$$l_{Dn}^2 = D_{\mathrm{n}}\tau_{\mathrm{n}}, \text{ the electron diffusion length}, \quad (11)$$
$$l_{Dp}^2 = D_{\mathrm{p}}\tau_{\mathrm{p}}, \text{ the hole diffusion length},$$
$$l_{\mathrm{Sn}} = \sqrt{\frac{\epsilon\epsilon_0 k_{\mathrm{B}}T}{e^2 N_{\mathrm{eff}}^{\mathrm{n}}}}, \text{ Debye screening length for electrons},$$
$$l_{\mathrm{Sp}} = \sqrt{\frac{\epsilon\epsilon_0 k_{\mathrm{B}}T}{e^2 N_{\mathrm{eff}}^{\mathrm{p}}}}, \text{ Debye screening length for holes}.$$

The standard characteristic times are

$$\tau_m^{\mathrm{n}} = \frac{\epsilon\epsilon_0}{\sigma_{\mathrm{n}}}, \text{ the dielectric relaxation time for electrons,}$$
$$\tau_m^{\mathrm{p}} = \frac{\epsilon\epsilon_0}{\sigma_{\mathrm{p}}}, \text{ the dielectric relaxation time for holes,}$$
$$\tau_{\mathrm{n}} = \frac{1}{\gamma_{\mathrm{n}}\bar{N}_1}, \text{ the moving electron lifetime,} \quad (12)$$
$$\tau_{\mathrm{p}} = \frac{1}{\gamma_{\mathrm{p}}(N_2 - \bar{N}_2)}, \text{ the moving hole lifetime .}$$

σ_{n} and σ_{p} are the electron and hole conductivities, respectively, D_{n} and D_{p} are the electron and hole diffusivities, respectively, $\bar{N}_1$ and $\bar{N}_2$ are the spatially uniform densities of the ionized centers 1 and 2, respectively, $N_{\mathrm{eff}}^{\mathrm{n}}$ and $N_{\mathrm{eff}}^{\mathrm{p}}$ are the effective trap densities for electrons and holes, respectively.

Equations (9) and (10) can be rewritten in a different way, more easy for the analysis:

$$\Gamma = \frac{1}{1+\tau_{\mathrm{f}}^2\Omega^2}\left(\Gamma_{\mathrm{f}} - \frac{\Gamma_{\mathrm{s}}}{1+\tau_{\mathrm{s}}^2\Omega^2}\right), \quad (13)$$
$$\Psi = -\frac{1}{2}\,\frac{1}{1+\tau_{\mathrm{f}}^2\Omega^2}\left(\Gamma_{\mathrm{f}}\tau_{\mathrm{f}}\Omega - \frac{\Gamma_{\mathrm{s}}\tau_{\mathrm{s}}\Omega}{1+\tau_{\mathrm{s}}^2\Omega^2}\right), \quad (14)$$

with the partial gain factors

$$\Gamma_{\mathrm{f}} = \frac{2\pi n^3 r_{\mathrm{eff}} E_{\mathrm{D}}}{\lambda(1+\ell_{\mathrm{Sn}}^2 K^2)}, \quad (15)$$
$$\Gamma_{\mathrm{s}} = \frac{2\pi n^3 r_{\mathrm{eff}} E_{\mathrm{D}}}{\lambda(1+\ell_{\mathrm{Sn}}^2 K^2)(1+\ell_{\mathrm{Sp}}^2 K^2)},$$

for the fast (subscript f) and slow (subscript s) gratings and the characteristic decay times

$$\tau_{\mathrm{f}} = \tau_m^{\mathrm{n}}\,\frac{1+\ell_{Dn}^2 K^2}{1+\ell_{\mathrm{Sn}}^2 K^2}, \quad (16)$$
$$\tau_{\mathrm{s}} = \tau_m^{\mathrm{p}}\,\frac{1+\ell_{Dp}^2 K^2}{1+\ell_{\mathrm{Sp}}^2 K^2}.$$

Note, that the amplitudes of the fast and slow grating are not independent in the case of SPS:

$$\Gamma_{\mathrm{f}} = \Gamma_{\mathrm{s}}(1+\ell_{\mathrm{Sp}}^2 K^2), \quad (17)$$

and for the small spatial freqiencies $\Gamma_{\mathrm{f}} \approx \Gamma_{\mathrm{s}}$.

The plots of (13) and (14) with the parameters of the particular sample of $Sn_2P_2S_6$ ($\Gamma_{\mathrm{f}}\ell = 5.8$; $\Gamma_{\mathrm{s}}\ell = 4.3$; $\tau_{\mathrm{f}} = 0.015$ s; $\tau_{\mathrm{s}} = 25$ s) are shown in Fig. 9. Figure 10 represents the same spectra in logarithmic plot to show more clearly the behavior near the gain maximum. As the log plot represents a part of the spectrum for $\Omega > 0$ only one of two peaks of the gain spectrum is visible in Fig. 10 a and only one (negative) spike appears in Fig. 10b roughly at $\Omega/2\pi \approx 0.005$ Hz.

Two symmetric maxima in the gain spectrum are well distinguished. It follows from (13) that the maximum gain is reached at

$$\Omega = \pm\sqrt{\frac{\Gamma_{\mathrm{s}}}{\Gamma_{\mathrm{f}}}\,\frac{1}{\tau_{\mathrm{f}}\tau_{\mathrm{s}}} - \frac{1}{\tau_{\mathrm{s}}^2}} \approx \pm\sqrt{\frac{1}{\tau_{\mathrm{f}}\tau_{\mathrm{s}}}}. \quad (18)$$

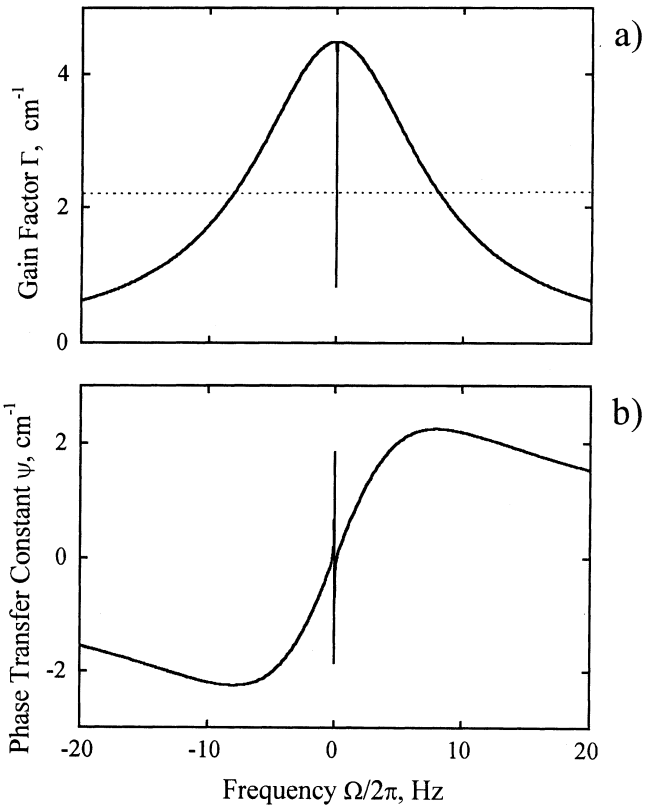

Fig. 9a,b. Calculated spectra of the gain factor (**a**) phase transfer constant (**b**). horizontal dots in (**a**) show the threshold level for coherent oscillation in the ring-loop cavity

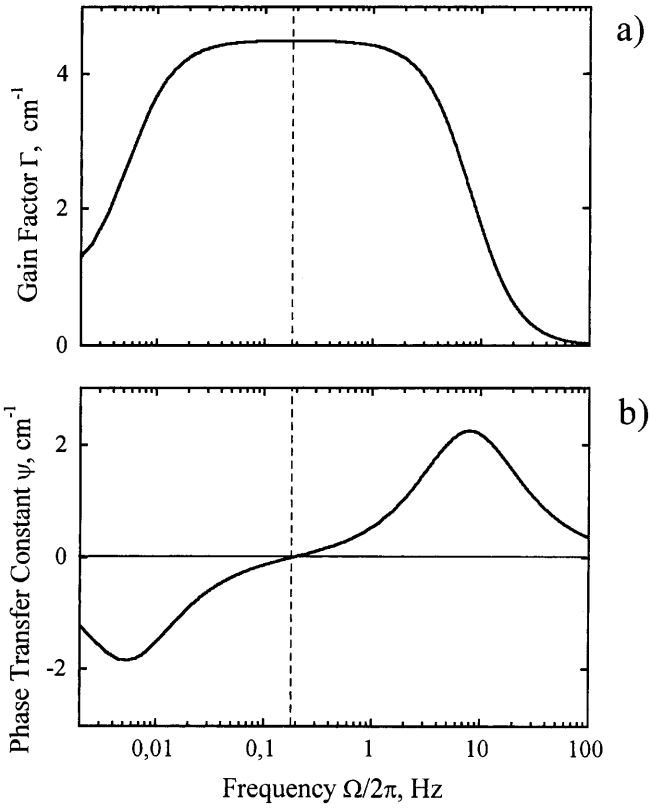

Fig. 10a,b. Detailed structure of gain spectrum (**a**) and phase transfer constant spectrum (**b**) for $Sn_2P_2S_6$ in the vicinity of zero detuning

Only one of the two relaxation times in (18) is intensity dependent, as the electron conductivity in (12) consists of the dark and photoconductivity:

$$\sigma_{\rm n} = \sigma_{\rm nd} + \kappa I_0, \tag{19}$$

κ being the specific photoconductivity. The hole conductivity $\sigma_{\rm p}$ in (12) is entirely defined by the thermally activated charge motion [16] and $\tau_{\rm s}$ is independent of the light intensity. Therefore we obtain from (18) rather unusual ($\sqrt{I_0}$) intensity dependence for the frequency separation of the gain maxima. On the other hand, both $\tau_{\rm f}$ and $\tau_{\rm s}$ are the functions of the grating spatial frequency (16); that is why the frequency separation will also depend on K.

2.2 Threshold conditions of oscillation

As for any other oscillator, to get the oscillation in a photorefractive coherent oscillator two conditions should be fulfilled [25, 26]. The *amplitude condition of oscillation* is the requirement that in one cavity round trip the gain should overcome the losses of all kinds. The *phase condition of oscillation* is, in fact, the condition of positive feedback: the phase of the oscillation wave should remain the same after one round trip of the cavity. Our aim is to find those detuning frequencies Ω for which both the amplitude and phase conditions of self-oscillation are fulfilled simultaneously and the difference $\Gamma(\Omega)\ell - (\Gamma\ell)_{\rm th}$ is maximized.

The theory of the coherent oscillator with the unclosed ring-loop cavity and ordinary photorefractive crystal possessing one dominant type of charge carriers [27] gives the amplitude condition of oscillation as follows:

$$(\Gamma\ell)_{\rm th} = \frac{2(R+1)}{R-1} \ln \frac{R+1}{2R}, \tag{20}$$

where ℓ is the sample thickness and R is the product of reflectivity of all cavity mirrors.

This condition is valid for a photorefractive crystal with purely nonlocal nonlinear response, i.e. for the $\pi/2$ shifted dynamic gratings. The nonlinear phase shift for the wave diffracted from the $\pi/2$ shifted grating is identically zero [24] (or π for the wave that is depleted in two-beam coupling configuration which is not of interest here). The absence of any dephasing in the diffracted wave ensures the phase condition of oscillation for the ring-loop configuration automatically. Two gratings, one recorded by the pump wave 2 (see Fig. 4) with the diffracted wave 3 and the other one recorded by the counterpropagating waves 1 and 4 are exactly in phase inside the photorefractive sample thus enhancing each other. This can be easily understood taking into account that waves 1 and 4 are in fact the waves 3 and 2 after passing the loop cavity once, i.e.,

$$\phi_1 = \phi_3 + k_{\rm os} L, \tag{21}$$

$$\phi_4 = \phi_2 + k_{\rm pump} L, \tag{22}$$

with k standing for wavenumber of the oscillaton (subscript "os") and pump (subscript "pump") waves and L for the loop length. With no non-reciprocity in the loop [26, 28] the phase difference $\phi_1 - \phi_4$ at the sample face facing the loop is exactly the same as $\phi_3 - \phi_2$ at the same face.

In the considered case of the coherent oscillator with SPS crystal the oscillation occurs at shifted frequency $\omega \pm \Omega$. This means that strictly speacking $k_{\rm os} \neq k_{\rm pump}$. The detuning frequency is nevertheless so small ($\Omega \approx 10^{-13}$–$10^{-14}\omega$) that for typical loop length 10–100 cm the resulting phase difference is negligibly small. More important is the other possible danger: usually the frequency detuning results in appearence of the local component in the nonlinear response and this leads to the nonlinear phase shift of the diffracted wave and to the bending of the interference fringes inside the sample (see, for example, [24]). As the angles of incidence of the pump wave and oscillation wave to the sample are interchanging after passing the cavity (see Fig. 4) the fringes from the waves 2, 3 and 1, 4 become bent in diffferent directions. This results in dephasing (violation of phase matching) and reduces the efficiency of the four-wave mixing.

Fortunately, for nondegenerate interaction in the crystal with π-out-of-phase gratings such as SPS, the contribution to the nonlinear phase shift in the vicinity of zero detuning from one grating will be opposite in sign with respect to the contribution from the other one. At a certain detuning frequency $\pm\Omega_{\rm max}$ these two contributions cancel each other exactly and the nonlinear phase shift becomes zero. This means that the coupling constant is real for these detuning frequencies, the fringes are not bent and the exact phase matching is restored.

It happens that the discussed detuning frequencies $\pm\Omega_{\rm max}$ just correspond to the maxima of the gain factor (see Fig. 10). This is not accidental; it has been shown recently [29] for several nonlinear effects that the real and imaginary nonlinear optical coefficients obey Kramers–Kronig relations in a similar way to the linear ones, ϵ' and ϵ''.

Thus we can conclude that $\pm\Omega_{\rm max}$ are the frequencies of two eigenmodes of this photorefractive oscillator. Still there is a third eigenmode with $\Omega = 0$ but it has nearly no chances to oscillate because of the much smaller gain factor for strictly degenerate interaction.

Note, that the frequencies $\pm\Omega$ depend on the total light intensity inside the sample I_0 and on the spatial frequency of the recorded grating K (see (16), (18)). The comparison of the experimental and calculated results is presented in the following section.

3 Discussion

The theory of the ring-loop coherent oscillator [27] predicts the threshold coupling strength $(\Gamma\ell)_{\rm th} = 2$ for a lossless cavity (with $R = 1$). Taking into account that the thickness of the SPS sample used in our experiment is $\ell = 0.9$ cm one can deduce from the gain spectrum (Figs. 9 and 10) that the amplitude condition of oscillation is fulfilled in a wide region of frequency detuning. At the same time the phase condition of oscillation is met only for $\Omega = 0$ and $\Omega = \pm\sqrt{\frac{1}{\tau_{\rm f}\tau_{\rm s}}}$ for the cavity with no non-reciprocity and for zero electric field (applied or internal). Thus our model predicts the coherent oscillation at two frequencies shifted symmetrically with respect to the pump wave frequency, in complete agreement with the experimental observation.

For high intensity of the pump wave (ensuring the photoconductivity much larger than the dark conductivity for carriers forming the "fast" grating) the frequency detuning of

the oscillation modes is proportional to the square root of the pump intensity ((12), (16), (18), (19)). The solid line in Fig. 7 is the best fit of the experimental dependence to the square root of intensity. An excellent qualitative agreement is quite evident. The quantitative discrepancy with the data calculated from known values of τ_s, τ_f, Γ_s, Γ_f is less than two times.

The characteristic decay times of two space-charge gratings are strongly dependent on spatial frequencies (Fig. 3); the time constant for the fast grating is decreasing with grating spacing while that for the slow grating grows with the grating spacing. As a result the calculated $1/\sqrt{\tau_f \tau_s}$ is nearly independent of the grating spacing. The slight increase of the frequency detuning with the grating spacing observed in the experiment may result from variation of the light intensity inside the sample: for a smaller angle between two beams their overlap is better and the cross section of the beam inside the sample is smaller. One should also take into account possible contribution to the discussed dependence of grating-spacing dependences for Γ_f and Γ_s (see (18)).

The onset of coherent oscillation here can be considered as the second-order optical phase transition, in a similar way to that described in [19, 30]. The infinite number of the "noisy" space-charge gratings with relatively small amplitudes self-develop in the sample below the threshold of oscillation, giving rise to the random light-induced scattering in a wide solid angle. Above the threshold two dominating gratings with the identical grating vectors appear, which couple all four interacting waves (incident pump wave, reflected by cavity mirrors pump wave, oscillation wave inside the cavity, and phase conjugate wave). The similarity to the "order–disorder" phase transition is quite obvious. Note, however, that for the considered optical oscillator the gratings that appear above the threshold are moving in the opposite direction with the same velocity. This results in the regular temporal variation of the amplitude of the space-charge grating and therefore in high contrast intensity modulation of the output oscillation. It is difficult to find a direct analogy for this kind of optical phase transition in solid-state physics: The periodic structures of atoms or molecules that appear there below the temperature of melting are stable in time.

4 Conclusions

A new steady-state oscillation mode consisting of simultaneous oscillation in two frequencies shifted symmetrically with respect to the pump frequency is revealed in SPS, photorefractive crystal with strong electron/hole competition. When the coupling strength $\Gamma(\Omega)\ell$ becomes larger than its threshold value given by (20) two space-charge gratings appear in the sample, moving in opposite directions with the velocities $\pm\Omega/K$. As a result the output of the oscillator has the high-contrast regular-intensity modulation. The modulation frequency, $2\Omega_{os}$, can be controlled by the intensity of the incident pump wave and by the spatial frequency of the space-charge grating (i.e., by the feedback loop angle near the sample). The calculations of the gain factor and phase transfer constant allow for good qualitative explanation of the experimental results.

Tin hypothiodiphosphate crystal is chosen for the experimental study as a typical material with the strong electron–hole competition. A similar behavior can be observed, however, in many other crystals with the pronounced space-charge compensation effects, such as, for example, recently described $Bi_4Ti_3O_{12}$ [5]. The slow grating, which is believed to build up in $Sn_2P_2S_6$ because of moving holes, can appear also because of ionic motion (in crystals with thermal fixing effect). A rather complete list of references for relevant materials is given in [5].

Acknowledgements. We thank Dr. K. Shcherbin for helpful discussions, Dr. A. Grabar and Dr. I. Stoyka for SPS samples, and our reviewers for helpful suggestions. Partial financial support of the Civilian Research and Development Foundation (UP2-322) and Ministry for Science, Technology and Industrial Politics, Ukraine (grant 4/356) is gratefully acknowledged.

References

1. E. Krätzig: Ferroelectrics **21**, 635 (1978)
2. R. Orlowski, E. Krätzig: Solid State Commun. **27**, 1351 (1978)
3. N. Barry, L. Duffault, R. Troth, R. Ramos-Garcia, M. Damzen: J. Opt. Soc. Am. B **11**, 1758 (1994)
4. E. Rickermann, S. Riehemann, K. Buse, D. Dirksen, G. von Bally: J. Opt. Soc. Am. B **13**, 2299 (1996)
5. X. Xue, E. Krätzig, R. Rupp: J. Opt. Soc. Am. B **15**, 2383 (1998)
6. S. Zhivkova, M. Miteva: J. Appl. Phys. **68**, 3099 (1990)
7. E. Strohkendl, J. Jonathan, R.W. Hellwarth: Opt. Lett. **11**, 312 (1986)
8. G. Valley: J. Appl. Phys. **59**, 3363 (1986)
9. M.C. Bashaw, M. Jeganathan, L. Hesselink: J. Opt. Soc. Am. B **11**, 1743 (1994)
10. M.C. Bashaw, T.-P. Ma, R.C. Barker: J. Opt. Soc. Am. B **9**, 1666 (1992)
11. G. Picoli, Ph. Gravay, C. Ozkul: Opt. Lett. **14**, 1362 (1989)
12. J.E. Millered, E.M. Garmire, M. Klein: Opt. Lett. **17**, 100 (1992)
13. S.G. Odoulov, A.N. Shumelyuk, G. Brost, K. Magde: Appl. Phys. Lett. **21**, 752 (1996)
14. A.N. Shumelyuk, S.G. Odoulov, G. Brost: J. Opt. Soc. Am. B **15**, 2125 (1998)
15. S.G. Odoulov, A.N. Shumelyuk, U. Hellwig, R.A. Rupp, A.A. Grabar: Opt. Lett. **21**, 752 (1996)
16. S.G. Odoulov, A.N. Shumelyuk, U. Hellwig, R.A. Rupp, A.A. Grabar, I.M. Stoyka: J. Opt. Soc. Am. B **13**, 2352 (1996)
17. A. Shumelyuk, S. Odoulov, Hu Yi, E. Krätzig, G. Brost: CLEO'98 Technical Digest, Paper CTuM58, p.171, OSA, San Francisco, 1998
18. M. Cronin-Golomb, B. Fischer, J.O. White, A. Yariv: Appl. Phys. Lett. **41**, 689 (1982)
19. D. Engin, S. Orlov, M. Segev, G.C. Valley, A. Yariv: Phys. Rev. Lett. **74**, 1743 (1995)
20. M.D. Ewbank, P. Yeh: Opt. Lett. **10**, 496 (1985)
21. M. Cronin-Golomb, A. Yariv: Opt. Lett. **11**, 242 (1986)
22. R. Eason, M. Gower: Opt. Commun. **59**, 77 (1986)
23. D. Gauthier, P. Narum, R. Boyd: Phys. Rev. Lett. **58**, 1640 (1987)
24. N.V. Kukhtarev, V.B. Markov, S.G. Odoulov, M.S. Soskin, V.L. Vinetskii: Ferroelectrics **22**, 949 (1979)
25. S. Odoulov, M. Soskin, A. Khyznyak: *Coherent oscillators with Four-Wave Mixing (Dynamic Grating Lasers)* (Harwood Academic Publichers, Chur, London 1989)
26. B. Fischer, S. Sternklar, S. Weiss: IEEE J. Quantum Electron. **QE-25**, 550 (1989)
27. M. Cronin-Golomb, B. Fischer, J.O. White, A. Yariv: IEEE J. Quantum Electron. **QE-22**, 12 (1984)
28. J.P. Jiang, J. Feinberg: Opt. Lett. **12**, 266 (1987)
29. D.C. Hutchings, M. Sheik-Bahae, D.J. Hagan, E.W. Van Stryland: Opt. Quantum Electron. **24**, 1 (1992)
30. M. Goul'kov, S. Odoulov, R. Troth: Ukr. Phys. J. **36**, 1007 (1991)